Determination of the orientation workspace of parallel manipulators

J-P. Merlet
INRIA Sophia-Antipolis
BP. 93
06902 Sophia-Antipolis Cedex, France

Abstract

An important step during the design of a parallel manipulator is the determination of its workspace. For a 6 d.o.f. parallel manipulator workspace limitations are due to the bounded range of their linear actuators, mechanical limits on their passive joints and links interference. The computation of the workspace of a parallel manipulator is far more complex than for serial link manipulator as its translation ability is dependent upon the orientation of the end-effector.

We present in this paper an algorithm enabling to compute the possible rotation of the end-effector around a fixed point. This algorithm enables to take into account all the constraints limiting the workspace. Various examples are presented.

Keywords: parallel manipulator, orientation workspace, workspace

1 Introduction

1.1 The mechanical structure of a parallel manipulator

Let us consider a 6 d.o.f. parallel manipulator as represented on Figure 1. It is constituted of a fixed base plate and a mobile plate connected by 6 extensible links. These legs are attached to the base and mobile plates with two- and three-degrees -of-freedom universal joints which makes the whole system be six-degrees-of-freedom.

This mechanical architecture is known since a long time and some of the theoretical problems it involves have been studied around 1900 [Bricard 97]. But working prototypes have been realized only recently as it seems that the first prototype can be attributed to Gough [Gough 57] in 1949.

This kind of robot has attracted a lot of interest in the 60's for the design of flight simulators [Stewart 65]. Indeed some of the main advantages of this kind of manipulator are their high nominal load and stiffness.

The use of parallel manipulators as robotics system is even more recent as the first one has been designed in 1979 [McCallion Pham 79]. In that case the point of interest is the high positionning accuracy. This feature explains why parallel manipulators have been used in robotics assembly cells [Fichter 86], [Arai Cleary +90], [Reboulet Pigeyre 90], [Pierrot 91]. But many theoretical problems remain to be solved, one of them being the determination of the workspace.

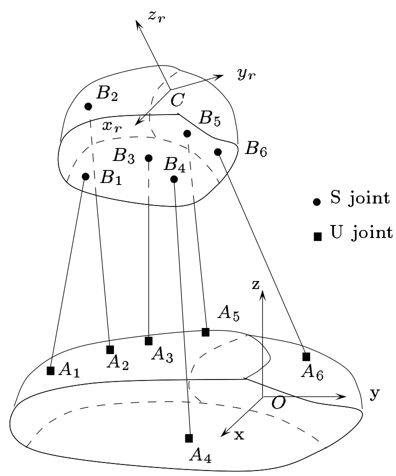

Figure 1: A 6 d.o.f. parallel manipulator.

1.2 Workspace representation

Determining the workspace of a robot is clearly an important step in the design phase. For serial link manipulators with decoupled wrist this workspace can be split in two 3D independent components: the possible positions of the center of the wrist which characterize the translation ability of the robot and the positions of the extreme point of the end-effector which will characterize the orientation ability.

The workspace of a parallel manipulator is limited due to three types of constraints:

- limited range for the link lengths. The minimum length of link i will be denoted ρ^i_{min} and the maximum length ρ^i_{max}
- mechanical limits on the passive joints (universal joints and ball and socket joints).
- links interference

The translation ability of a parallel manipulator is clearly dependent upon the orientation of the end-effector. This imply that a full representation of the workspace would have to be done in a six-dimension space for which there is no human representation.

Fortunately in many applications the robot is used either with a fixed orientation or rotates around a fixed point. This means that among the six generalized coordinates of the end-effector at least three of them have a constant value. In this paper we will consider that one point of the end-effector is fixed in the reference frame.

2 Notation

We define first two frames, one fixed (reference frame) and the other one attached to the end effector (relative frame).

The following symbols and variables will be used in this paper:

- A_i: center of the passive joint of link i attached to the base of the robot.
- B_i: center of the passive joint of link i attached to the end effector.
- O: origin of the reference frame

- x, y, z: axis of the reference frame
- C: origin of the relative frame.
- x_r, y_r, z_r: axis of the relative frame. The z_r axis is directed along the normal to the mobile plate.
- ψ, θ, ϕ: Euler's angles defining the orientation of the end effector
- ρ^i: length of link i

If there is no ambiguity the subscripts will be omitted. A superscript ^{r} will be used for vectors whose coordinates are expressed in the relative frame.

2.1 State of the art

In most of the works dealing with workspace determination it is assumed that the orientation of the end-effector is fixed. In that case only the possible translations of the end-effector are to be determined.

For solving this problem many authors use a discretization method in the parameter's space [Arai Cleary $^+$90], [Cleary Arai 91],[Fichter 86],[Lee Shah 88],[Merlet 87]. Discretization methods are usually time expensive and not very efficient.

Another approach has been proposed by some authors [Jo Haug 89] [Agrawal 91],[Landsberger Shanmugasundram 92] It is based on the fact that for a point on the border of the workspace the velocity of the manipulator along the normal to the border must be equal to zero. But this method imply the use of the jacobian matrix of the robot for which no closed-form is known. Furthermore this method is not convenient to introduce the constraints of links interference and mechanical limits on the passive joints.

A completely different approach has been proposed by C.Gosselin [Gosselin 89] which uses a purely geometrical method for determining the workspace border due to the limited range of the links lengths. This approach has then been extended to take into account all the constraints limiting the workspace [Merlet 92] enabling to calculate exactly and quickly border of cross-sections of the workspace.

As for the orientation workspace of 6 d.o.f manipulators few works has been done, most of them using a discretization method [Pooran 89], [Merlet 90]. Weng [Weng 88] has proposed for a specific manipulator a differential approach to compute the dextrous workspace i.e. the set of positions of the center of the end-effector where any orientation is allowed. But the only constraint which are taken into account are the link lengths: this is a main drawback as links interference will clearly play an important role for limiting the rotation of the end-effector.

In the planar case Pennock [Pennock Kassner 91] and Williams [Williams II Reinholtz 88] have addressed this problem especially to find the maximal workspace i.e. the set of positions of the end-effector which can be reached with at least one orientation. But their methods cannot be extended for 6 d.o.f. robot.

3 Orientation workspace

3.1 Introduction

In this paper we will assume that the center C of the relative frame is fixed in the reference frame and we will try to determine what are the allowed rotations of the end-effector around this point.

Representing the orientation of a rigid body is somewhat difficult. Plotting the three angles defining this orientation (for example the three Euler's angles) does not lead to a very understandable representation. Therefore we will introduce another form of representation.

We consider a unit link $\mathbf{N} = CN_e$ attached to the end-effector at point C. As the end-effector rotates around C the extremity N_e of the link moves on the unit sphere centered at C. If the end-effector can rotate freely point N_e will describe the whole unit sphere. If there are some restrictions on the rotation of the end-effector point N_e will describe only some regions on the unit sphere. Therefore if we are able to compute the border of the regions described by N_e during the possible rotations of the end-effector we will have characterized the possible rotations with the exception of the rotations around the unit link. Hence such a representation enables to describe two rotational degrees of freedom of the robot. By choosing carefully the direction of the unit link we will be able to represent all the possible rotations of the end-effector.

We will assume that we rotate first the end-effector around a fixed vector $\mathbf{X_1}$ with an angle θ_1. We then investigate the possible rotation of the end-effector around a given vector $\mathbf{X_2}$ in the reference frame. During this rotation the extremity N_e of $\mathbf{N}$ describes a circle C_e on the unit sphere in a plane perpendicular to $\mathbf{X_2}$ (Figure 2). The constraints on the manipulator imply that N_e may lie only on some

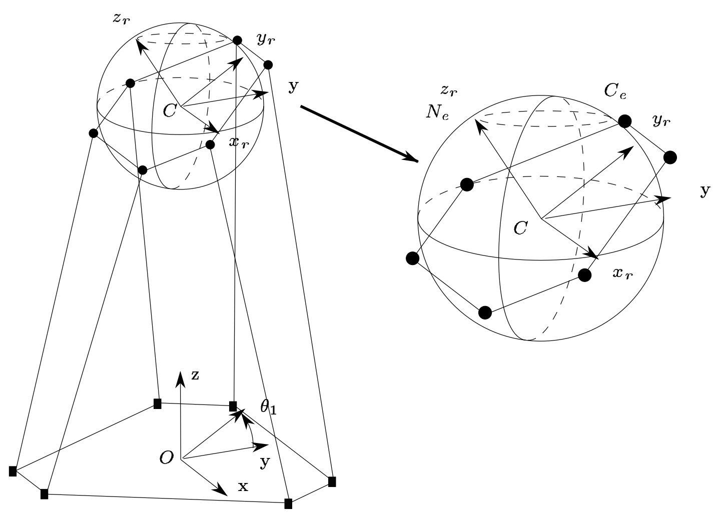

Figure 2: Example of end-effector rotation. Here the unit link attached to the end-effector at C is directed along z_r. The end-effector has been rotated around the axis x with an angle θ_1 ($\mathbf{X_1} = [1, 0, 0]$). In this configuration when the end-effector rotates around the axis z ($\mathbf{X_2} = [0, 0, 1]$) point N_e describes a circle on the unit sphere (the ellipsis in dashed line)

parts of the circle C_e. The purpose of our algorithm is to determine these allowed parts. By computing these allowed parts for various values of θ_1 the set of circles C_e will span approximatively the unit sphere and we will get the possible regions for N_e on the sphere and therefore the orientation workspace of the robot.

3.2 Workspace limitation due to the link lengths

3.2.1 Allowable zones for B_i

As the end-effector rotates around C point B_i lie on a sphere S_{C_i} with center C and radius $||CB_i||$. Point B_i must also lie in a volume whose borders are the spheres S_{e_i}, S_{i_i} centered in A_i with radii $\rho^i_{min}, \rho^i_{max}$, the minimum and maximum value of the leg length (Figure 3). Consequently the allowed zone Z_{B_i} for B_i on S_{C_i} is limited by the two circles C_{e_i}, C_{i_i} which are the intersection circles of the sphere S_{C_i} with the spheres S_{e_i}, S_{i_i}. For a given rotation angle of the end-effector around $\mathbf{X_1}$ as the end-effector rotates around $\mathbf{X_2}$ point B_i will describe a circle C_{B_i} (Figure 4). Note that the circles $C_{e_i}, C_{i_i}, C_{B_i}$ can be easily deduced from the geometry of the robot.

Two cases may occur: either the circle C_{B_i} has no intersection with the circles C_{e_i}, C_{i_i} or the circle C_{B_i} has at least one common point with C_{e_i}, C_{i_i}

In the first case the circle C_{B_i} is either fully inside the zone defined by the circles C_{e_i}, C_{i_i} (case 1 on Figure 4) and therefore the allowable zone for point B_i is the full circle C_{B_i} or the circle C_{B_i} is fully

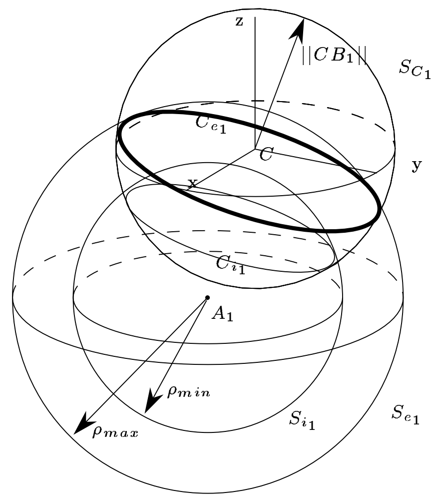

Figure 3: For any rotation around C point B_1 lie on the sphere S_{C_1} centered in C with radius $||CB_1||$. This point must also lie inside the volume defined by the spheres S_{e_1}, S_{i_1} centered in A_1 with radii $\rho^1_{min}, \rho^1_{max}$

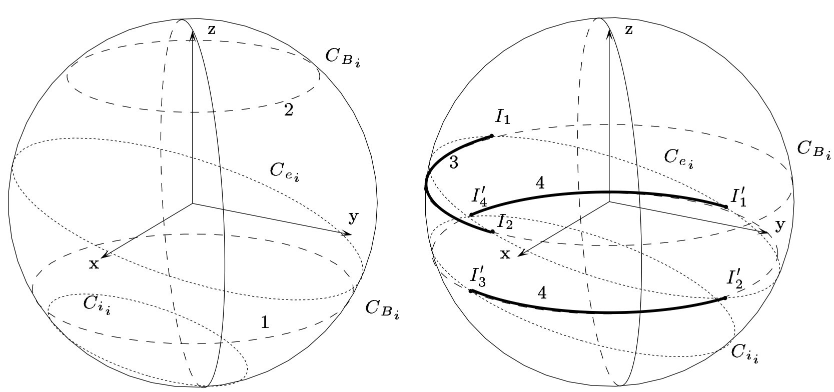

Figure 4: For given rotation angle of the end-effector around $\mathbf{X_1}$ point B_i describes a circle C_{B_i} (in dashed line) when the end-effector rotates around $\mathbf{X_2}$. If C_{B_i} lie inside the zone defined by the two circles C_{e_i}, C_{i_i} (in thin dashed line) B_i can lie on the whole circle (1). At the opposite if C_{B_i} is completely outside the zone no rotation is allowed (2). If C_{B_i} has intersection points with C_{e_i}, C_{i_i} only some parts of C_{B_i} are allowed for B_i (drawn in thick line on the right).

outside the zone (case 2 on Figure 4) in which case no rotation of the end-effector is allowed. These cases can be distinguished by taking any arbitrary point on the circle C_{B_i} (the orientation of the end-effector is therefore fully determined) and computing the link length for this point: if the length is inside the link length range the whole circle C_{B_i} is allowed.

Suppose now that there exist intersection points of C_{B_i} with at least one of the circles C_{e_i}, C_{i_i}.

We will have either two intersection points I_1, I_2 (C_{B_i} intersects only one of the circles, case 3 on Figure 4) or four intersection points $I'_{1..4}$ (case 4 on Figure 4). These intersection points define arcs of circle on C_{B_i}. For a point on a given arc the link length is either always in the link length range or is always outside this range. Therefore we consider each arc and determine if the arc defines an allowable zone for B_i on C_{B_i} by taking an arbitrary point on the arc (usually the middle point of the arc) and verifying if the link length for this position is in the link length range.

After completing this test for all the arcs we get the set of all allowable zone for B_i on C_{B_i}.

3.2.2 Allowable zones for N constrained by link i

As the end-effector rotates around $\mathbf{X_2}$ point N_e describes a circle C^N on the unit sphere. Let us assume now that we have determined the allowed arcs for the point B_i on its circle C_{B_i}. Clearly when B_i describes one of these arcs A^i_j N_e describes an arc of circle $\mathcal{A}^i_j$, part of C^N. For any configuration of the end-effector defined by a position of N_e on this arc the length of link i is inside its range. Therefore $\mathcal{A}^i_j$ defines an allowable zone for N_e for link i.

Consequently we have to determine the extremities of $\mathcal{A}^i_j$ for a given arc A^i_j described by B_i. Assume that point B_i is located at one of the extremity of A^i_j. For this location of B_i the orientation of the end-effector is completely determined and we denote by R_e the corresponding rotation matrix. We have :

$$\mathbf{N} = \mathbf{CN_e} = \mathbf{CB_i} + \mathbf{B_iN_e} \tag{1}$$

Let $\mathbf{CN^r_e}$ be the relative coordinates of N_e and $\mathbf{CB^r_i}$ the relative coordinates of B_i. We may thus write:

$$\mathbf{B_iN_e} = R_e\mathbf{CN^r_e} - R_e\mathbf{CB^r_i} \tag{2}$$

By combining equations (1) et (2) we get:

$$\mathbf{N} = \mathbf{CB_i} + R_e(\mathbf{CN^r_e} - \mathbf{CB^r_i}) \tag{3}$$

Equation (3) enables to compute $\mathbf{N}$ (and therefore the location of N_e) for a given location of B_i. Consequently we can calculate the position of the extremities of the arc $\mathcal{A}^i_j$ corresponding to the extremities of the arc A^i_j. This enables to compute the arcs of circle for N_e on C^N for which the constraints on the length of link i are satisfied.

3.2.3 Allowable zones for N constrained by all the links

For a fixed rotation around $\mathbf{X_1}$ point N_e describes a circle C^N and we have determined in the previous section the arc of circle on C^N for which the link length constraints for one link are satisfied. By computing these arcs for all the links and calculating their intersection we are able to determine the arcs of circle for which the lengths of the legs are within their allowed ranges and consequently the allowed zones on C^N for this kind of constraint.

By computing these zones for various values of θ_1 in the range $[0, 2\pi]$ we will get a good approximation of the allowable zone for N_e on the unit sphere.

Note however that we have to separate the interval of variation on θ_1 in two componants as there are two values of θ_1 such that N_e will describe the same circle C^N. For example if $\mathbf{N}$ is directed along the normal to the end-effector, $\mathbf{X_1}$ being the x axis then θ_1 and $-\theta_1$ lead to the same circle for N_e.

An example of computation of the allowable zones for N_e is presented in Figure 5 for the manipulator described in the appendix.

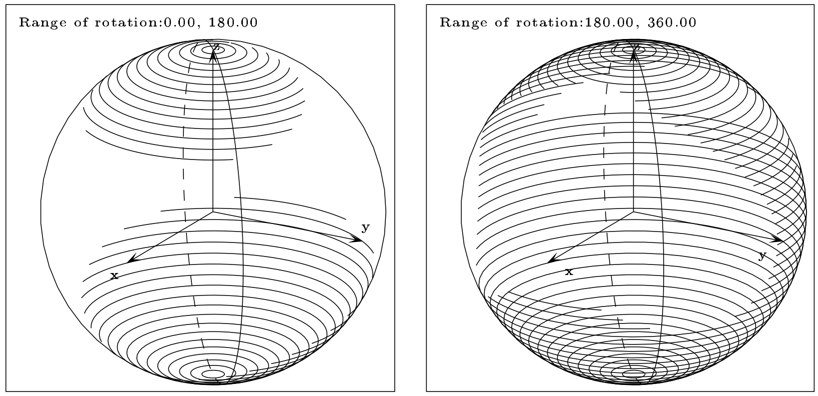

Figure 5: In thin lines the allowable zones for an unit link directed along the z_r axis of the mobile plate when the mobile plate rotates around the z axis after being first rotated around the x axis. On the left the angle of rotation around x is in the range $[0,\pi]$ and on the right in the range $[\pi, 2\pi]$. The constraints limiting the rotation are the link lengths.

3.3 Mechanical limits on the passive joints

The mechanical limits on joints like universal joints or ball-and-socket joints can be modelized by a surface which is the border of the allowable zone for the link connected to the joint. Using a similar method as in [Merlet 92] we assume that this surface can be approximated by a pyramid with planar faces. For the joints attached to the base the center of this pyramid is located at point A (Figure 6).

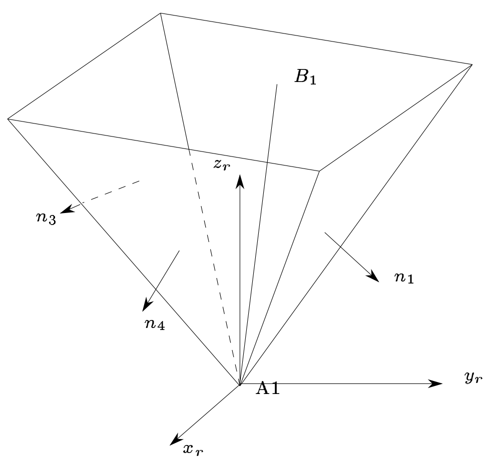

Figure 6: An example of modelization of a constraint on a passive joint located at A_1. If the mechanical limits of the joints are satisfied then link A_1B_1 is inside the volume delimited by the pyramid.

As for the constraints on the passive joints attached to the end-effector we may use the same model. We define a pyramid P_i with center B_i such that if the constraint on the joint at B_i are satisfied then point A_i lie inside the pyramid (figure 7, left). From this pyramid we deduce an *equivalent pyramid* $P_i^,$ to P_i, whose center is A_i, such that if A_i lie inside P_i then B_i lie inside $P_i^,$ (figure 7, right).

We consider the intersection points of the circle C_{B_i} described by B_i with the faces of the pyramid describing the constraints on the joint at A_i. These intersection points, if any, define arcs of circle on C_{B_i}

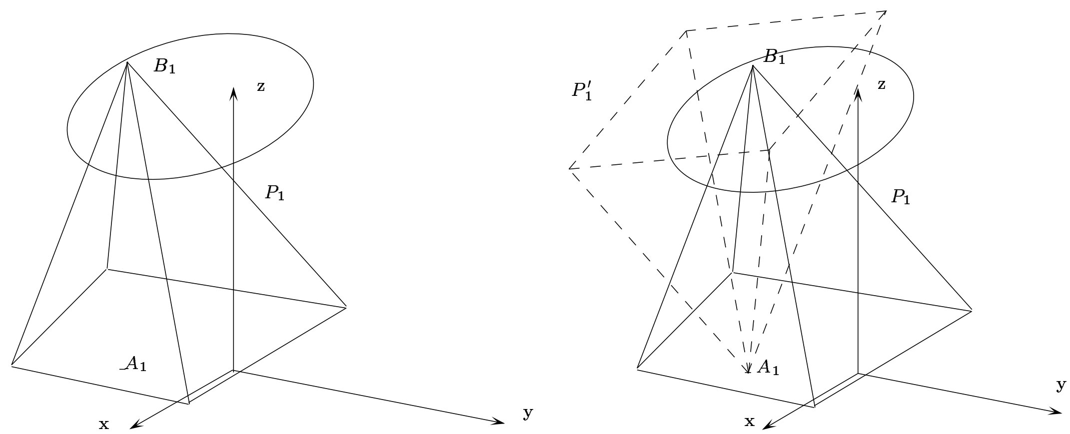

Figure 7: Modelization of the constraint on the joint at B: if the mechanical limits on the joint are satisfied the point A_1 lie inside a pyramid (left). From this pyramid we deduce an equivalent pyramid P_1' centered at A_1 such that if the mechanical limits on the joint are satisfied then point B_1 lie inside P_1' (right).

such that for any position of B_i on the arc either the link A_iB_i is fully inside the pyramid (the constraint on the joint are therefore satisfied) or some part of the link lie outside the pyramid. For each of these arcs we take an arbitrary point on the arc (usually the middle point of the arc) and test if the link is inside the pyramid for this position of B_i. If this is true then the arc is an allowable region for B_i from the view point on the constraints on the joint (Figure 8). A similar algorithm is used with the equivalent

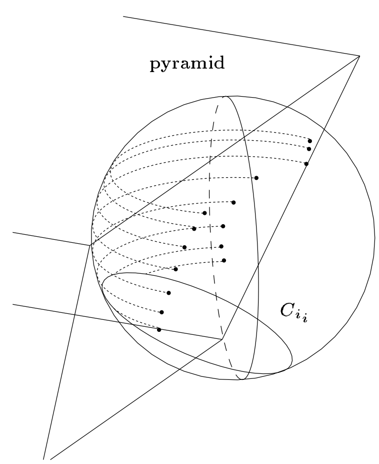

Figure 8: The intersection points of the circles C_{B_i} and the pyramid (dotted points) enable to compute the arcs (in dashed line) of the C_{B_i}'s such that the passive joints constraints are satisfied.

pyramid to find the allowable region for B_i from the view point on the constraints on the joint at B_i.

From the allowable regions for B_i we deduce in a similar manner as for the link lengths constraints the allowable regions $\mathcal{A}^j_{A_iB_i}$ for N_e on C^N due to the constraints on the joints.

At this point we have computed a set $\mathcal{A}^j_i$ of arcs on C^N for which the link lengths constraints are satisfied and a set $\mathcal{A}^j_{A_iB_i}$ of arcs on C^N such that the constraints on the joints at A_i, B_i are satisfied.

The intersection of each arc in the set $\mathcal{A}_i^j$ with the set $\mathcal{A}_{A_iB_i}^j$ defines the arcs on which all the constraints are satisfied (Figure 9).

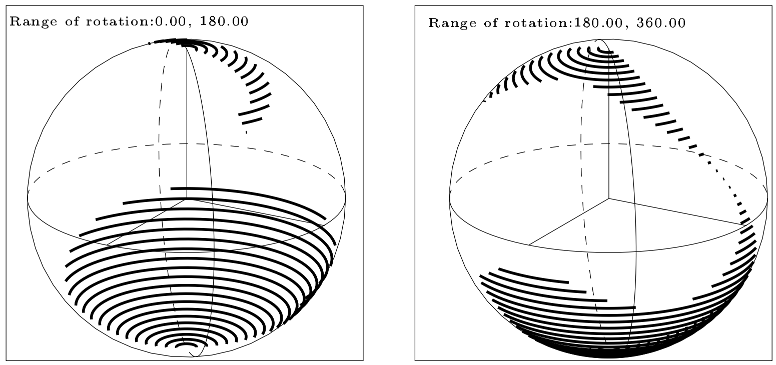

Figure 9: For the manipulator described in the appendix we have determined the allowable region for for the extremity of an unit link directed along the z_r axis of the mobile plate when the mobile plate rotates around the z axis after being first rotated around the x axis. On the left the angle of rotation around x is in the range [0,π] and on the right in the range $[\pi, 2\pi]$. The constraints limiting the rotation are the link lengths and the constraints on the base joints.

3.4 Links interference

An important factor limiting the rotation of the mobile plate is clearly the links interference.

We define the distance between two links as the minimal distance between any pair of points on the links. It has been shown in [Merlet 92] that the distance between link $, i, j$ is the minimum of the following quantities:

- the distance between the lines associated to the links if their common perpendicular has a point on each link
- the distance between a point B and its projection B^p on the other link if B^p belongs to the link
- the distance between a point A and its projection A^p on the other link if A^p belongs to the link
- the distance between the points of one of the two pairs of points (A_i, B_j)

The notion of distance between the links is illustrated in Figure 10.

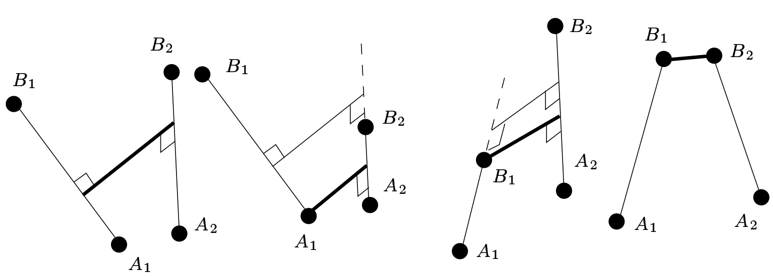

Figure 10: Distance between two links.

We assume that each link i can be approximated by a cylinder with radius r_i and will say that links i, j interfere if their distance if lower than $d = r_i + r_j$.

We will consider without loss of generality only links 1 and 2 and will assume that the distance between A_1, A_2 and B_1, B_2 is greater than d (in the opposite case the links will always interfere).

We define d_{ij} as the distance between the lines associated to the links i, j, $d(A, B)$ as the distance between the points A, B. $P^j_{M_i}$ denotes the projection of a point M belonging to link i on link j and P_i, P_j the points of lines i, j belonging to the common perpendicular of lines i, j.

For a given rotation angle θ_1 around $\mathbf{X_1}$ we want to determine the location of the point B_i such that the distance between the links i, j is equal to $r_i + r_j$. Therefore we have to find the rotation angles θ_2 such that one of the following relations is satisfied:

$$\left\{\begin{array}{lll} d_{ij} = d(P_i, P_j) & = r_i + r_j \text{ with } \quad P_i \in A_iB_i \quad P_j \in A_jB_j & \\ d(A_i, P^j_{A_i}) & = r_i + r_j \text{ with } P^j_{A_i} \in A_jB_j & d(A_i, B_j) = r_i + r_j \\ d(B_i, B_j) & = r_i + r_j & d(B_i, A_j) = r_i + r_j \\ d(A_j, P^i_{A_j}) & = r_i + r_j \text{ with } P^i_{A_j} \in A_iB_i & d(B_i, P^j_{B_i}) = r_i + r_j \text{ with } P^j_{B_i} \in A_jB_j \\ d(B_j, P^i_{B_j}) & = r_i + r_j \text{ with } P^i_{B_j} \in A_iB_i & d(A_i, A_j) = r_i + r_j \end{array}\right. \tag{4}$$

All the relations defined by (4) have the same form and can be written as:

$$a_1 \sin(\theta_2) + a_2 \cos(\theta_2) + a_3 = 0 \tag{5}$$

where the a_i coefficients are dependent only from the relation and the geometry of the robot. This kind of equation leads at most to two solutions in θ_2 i.e. two locations for the point B_i on the circle C_{B_i} such that the distance between link i and link j is equal to d.

For the analysis of the possible positions of the point B_i on the circle C_{B_i} with respect to links interference we will compute the set of points on C_{B_i} such that the distance between links i, j is equal to $d = r_i + r_j$. This set is determined through the equations (5) and an example is shown in Figure 11. Therefore on the circle C_{B_i} we get various set of *critical points*:

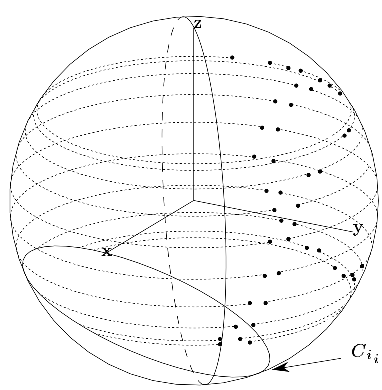

Figure 11: At some points on C_{B_i} the distance between link i and another link j is equal to $r_i + r_j$ (dotted points)

- the intersection points of C_{B_i} with the circles C_{e_i}, C_{i_i}
- the intersection points of C_{B_i} with the faces of the pyramids describing the constraints on the joints centered at A_i, B_i
- the set of points such that the distance between links i, j is equal to $r_i + r_j$

This set of critical points defines various arcs on C_{B_i}. We consider each of these arcs of circle and test if the whole set of constraints is satisfied for one specific point of the arc (usually the middle point). If this test is true then the arc is an allowable regions for B_i. From the set of allowable regions for B_i we deduce a set of allowable regions $\mathcal{A}_i^{N_e}$ for N_e for which the constraints on link i are satisfied. Then the intersection of the six $\mathcal{A}_i^{N_e}$ defines the allowable region for N_e on C^N.

Figures 12,13 show for example the possible regions for an unit link directed along the y axis when the mobile plates rotates around the x, z axis: this illustrate the possible rotation of the end-effector around the z axis. Clearly a full rotation around this axis is not possible as links interference will occur. It may be seen that if links interference is not considered some of the circles C^N can be completely described by N_e: the leg lengths ranges and mechanical limits on the passive joints enable theoretically a full rotation. But as soon as links interference is taken into account the same circles are split in smaller componants: links interferences have been detected.

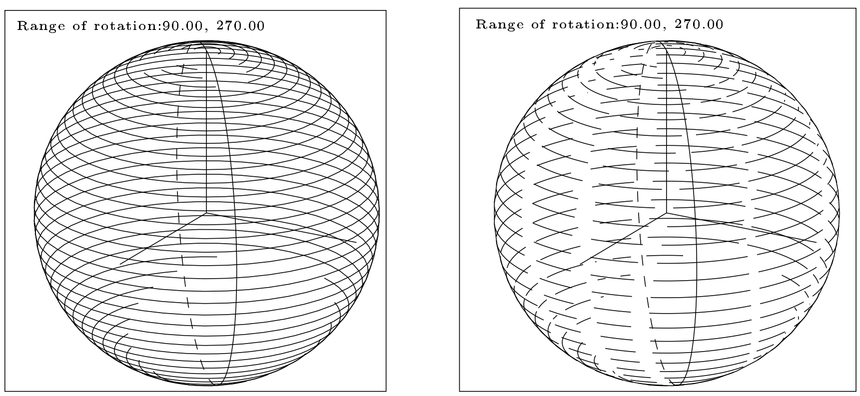

Figure 12: In thin line the allowable zones for an unit link directed along the $-y_r$ axis of the mobile plate when the mobile plate rotates around the z axis after being first rotated around the x axis with a rotation angle in the range $[\pi/2 - 3\pi/2]$. On the left the constraints are only the link lengths and on the right links interference have been taken into account.

4 Conclusion

The algorithm presented in this paper enables to compute and represent two of the three possible rotations of the end-effector around a fixed point. This is done by computing the reachable regions of the extremity of a fixed-length link attached to the mobile plate. This algorithm takes into account all the constraints limiting the orientation workspace: links lengths range, mechanical limits on the passive joints, links interference. As this method is purely geometrical it imply few calculations: consequently this leads to a very fast and efficient algorithm.

We plan to extend this algorithm for computing the maximal workspace of parallel manipulator.

5 Appendix: The manipulator and some examples

One of the prototype of parallel manipulator developed at the Mechanical Engineering Laboratory of Tsukuba [Arai Cleary +90] has been considered for this study.

In this prototype the base joints are located under the base plate and the links go through a square opening. We can therefore modelize the joint constraints by a four-faced pyramid.

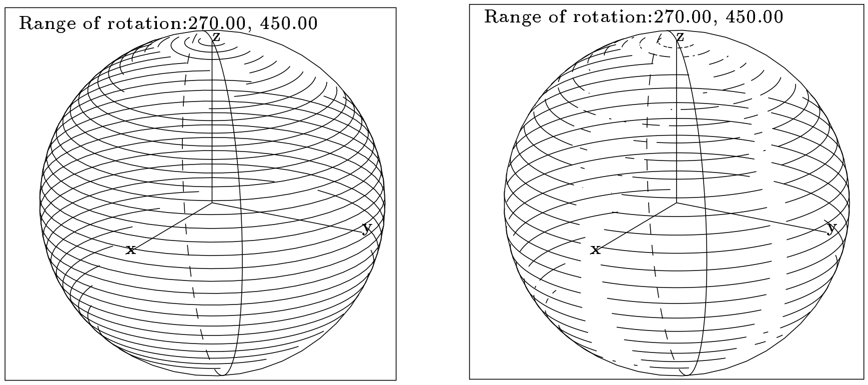

Figure 13: In thin line the allowable zones for an unit link directed along the $-y_r$ axis of the mobile plate when the mobile plate rotates around the z axis after being first rotated around the x axis with a rotation angle in the range $[3\pi/2 - \pi/2]$. On the left the constraints are only the link lengths and on the right links interference have been taken into account.

The position of the joints centers and the minimum and maximum links lengths are given in Figure 14. We may notice that the joints have a disposition which imply some risks of links interference.

Link	1	2	3	4	5	6
x_a	112.5	-225	-112.5	67.5	-135	67.5
y_a	-194.856	0	194.856	-116.913	0	116.913
z_a	-25	-25	-25	-25	-25	-25
x_b	95.263	0	-95.263	-69.282	0	69.282
y_b	55	-110	55	-40	80	-40
z_b	-20	-20	-20	-20	-20	-20
ρ_{max}	757	757	757	733	733	733
ρ_{min}	528	528	528	491	491	491

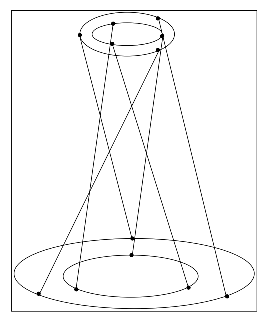

Figure 14: Position of the base and mobile joints centers and minimum and maximum links lengths (in mm)

The figures represent the orientation workspace for a unit link directed along the normal of the mobile plate for rotations first around the x axis then around the z axis.

In Figure 15 the constraints are only the link lengths, in Figure 16 we have added the constraints on the base joints and in Figure 17 links interferences have also been considered (link radius: 8mm). The allowable regions for N_e are drawn in grey.

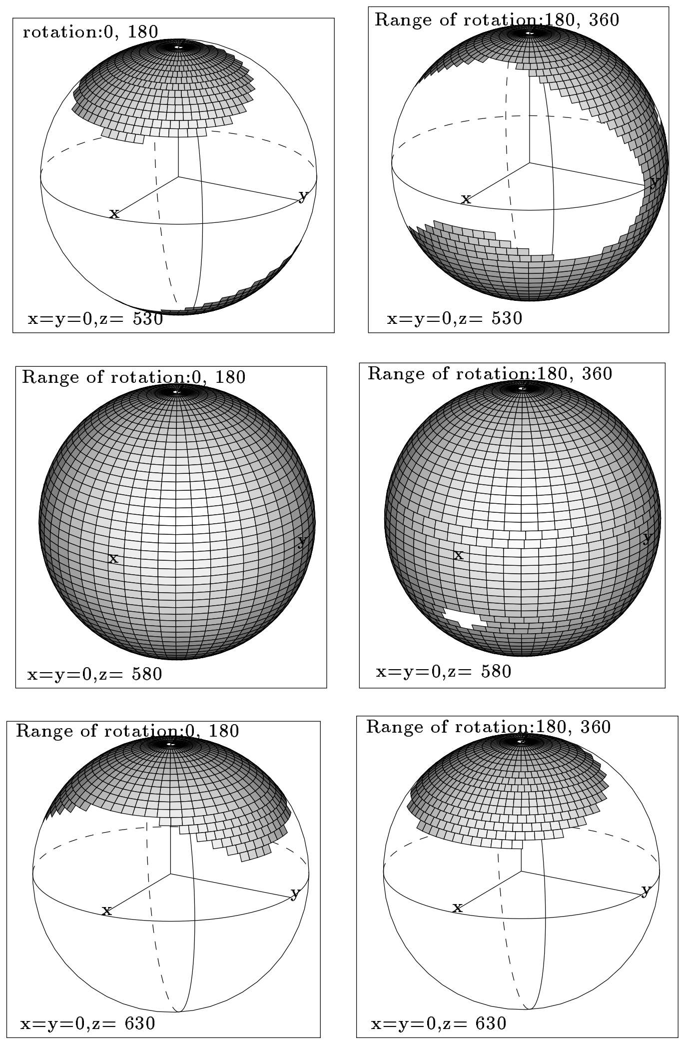

Figure 15: Representation of the possible regions for the extremity of an unit link directed along the z_r axis of the mobile plate when the mobile plate rotates around the z axis after being first rotated around the x axis. The constraints are only the link lengths.

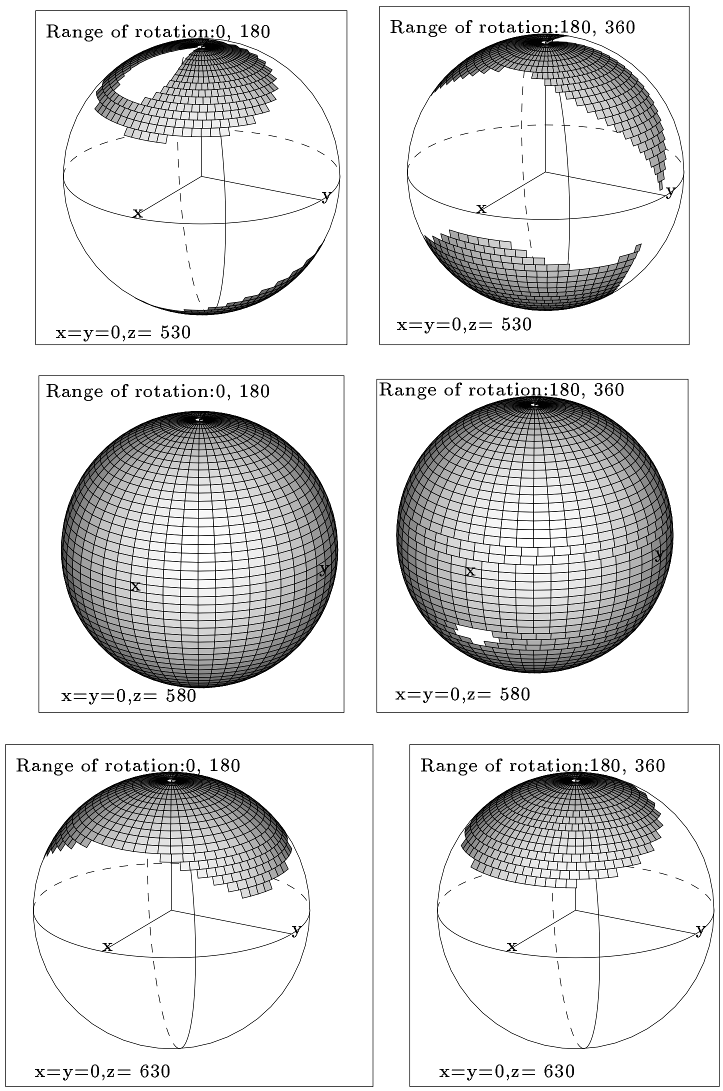

Figure 16: Representation of the possible regions for the extremity of an unit link directed along the z_r axis of the mobile plate when the mobile plate rotates around the z axis after being first rotated around the x axis. The constraints are the link lengths and the constraints on the base joints.

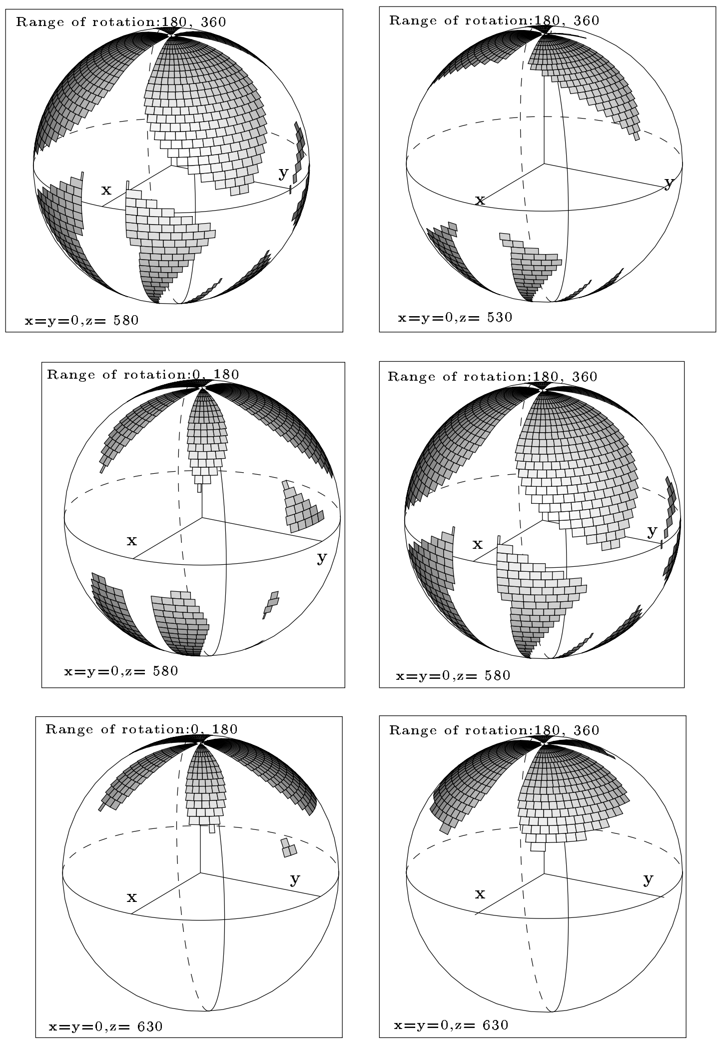

Figure 17: Representation of the possible regions for the extremity of an unit link directed along the z_r axis of the mobile plate when the mobile plate rotates around the z axis after being first rotated around the x axis. The constraints are the link lengths, the constraints on the base joints and links interference.

References

[Agrawal 91] Agrawal S.K. Workspace boundaries of in-parallel manipulator systems. In *ICAR*, pages 1147–1152, Pise, June, 19-22, 1991.

[Arai Cleary +90] Arai T., Cleary K., and others . Design, analysis and construction of a prototype parallel link manipulator. In *IEEE Int. Workshop on Intelligent Robots and Systems (IROS)*, volume 1, pages 205–212, Ibaraki, Japan, July, 3-6, 1990.

[Bricard 97] Bricard R. Mémoire sur la théorie de l'octaèdre articulé. *Journal de Mathématiques pures et appliquées, Liouville*, tome 3:113–148, 1897.

[Cleary Arai 91] Cleary K. and Arai T. A prototype parallel manipulator: kinematics construction, software, workspace results and singularity analysis. In *IEEE Int. Conf. on Robotics and Automation*, pages 566–571, Sacramento, April, 11-14, 1991.

[Fichter 86] Fichter E.F. A Stewart platform based manipulator: general theory and practical construction. *Int. J. of Robotics Research*, 5(2):157–181, Summer 1986.

[Gosselin 89] Gosselin C. Determination of the workspace of 6-dof parallel manipulators. In *ASME Design Automation Conf.*, pages 321–326, Montréal, September, 17-20, 1989.

[Gough 57] Gough V.E. Contribution to discussion of papers on research in automobile stability, control and tyre performance, 1956-1957. Proc. Auto Div. Inst. Mech. Eng.

[Jo Haug 89] Jo D.Y. and Haug E.J. Workspace analysis of closed loop mechanisms with unilateral constraints. In *ASME Design Automation Conf.*, pages 53–60, Montréal, September, 17-20, 1989.

[Landsberger Shanmugasundram 92] Landsberger S.E. and Shanmugasundram A.P. Workspace of parallel link crane. In *IMACS/SICE Int. Symp. on Robotics, Mechatronics, and Manufacturing Systems*, pages 479–486, Kobe, September, 16-20, 1992.

[Lee Shah 88] Lee K-M and Shah D.K. Kinematic analysis of a three-degrees-of-freedom in-parallel actuated manipulator. *IEEE J. of Robotics and Automation*, 4(3):354–360, June 1988.

[McCallion Pham 79] McCallion H. and Pham D.T. The analysis of a six degrees of freedom work station for mechanized assembly. In *Proc. 5th World Congress on Theory of Machines and Mechanisms*, pages 611–616, Montréal, July 1979.

[Merlet 87] Merlet J-P. Parallel manipulators, Part 1, theory. Technical Report 646, INRIA, March 1987.

[Merlet 90] Merlet J-P. *Les Robots parallèles*. Hermès, Paris, 1990.

[Merlet 92] Merlet J-P. Geometrical determination of the workspace of a constrained parallel manipulator. In *ARK*, pages 326–329, Ferrare, September, 7-9, 1992.

[Pennock Kassner 91] Pennock G.R. and Kassner D.J. The workspace of a general geometry planar three degree of freedom platform manipulator. In *ASME Design Automation Conf.*, pages 537–544, Miami, September, 22-25, 1991.

[Pierrot 91] Pierrot F. *Robots Pleinement Parallèles Légers : Conception Modélisation et Commande.* PhD thesis, Université Montpellier II, Montpellier, April, 24, 1991.

[Pooran 89] Pooran F.J. *Dynamics and control of robot manipulators with closed-kinematic chain mechanism.* PhD thesis, The Catholic University of America, Washington D.C., 1989.

[Reboulet Pigeyre 90] Reboulet C. and Pigeyre R. Hybrid control of a 6 d.o.f. in parallel actuated micro-macro manipulator mounted on a Scara robot. In *ISRAM*, volume 3, pages 293–298, Burnaby, July, 18-20, 1990. ASME Press Series.

[Stewart 65] Stewart D. A platform with 6 degrees of freedom. *Proc. of the Institution of mechanical engineers*, 180(Part 1, 15):371–386, 1965.

[Weng 88] Weng T.C. *Kinematics of parallel manipulators with ground-mounted actuators.* PhD thesis, University of Florida, Gainesville, 1988.

[Williams II Reinholtz 88] Williams II R.L. and Reinholtz C.F. Closed-form workspace determination and optimization for parallel robot mechanisms. In *ASME Proc. of the the 20th Biennial Mechanisms Conf.*, pages 341–351, Kissimmee, Orlando, September, 25-27, 1988.